ELSEVIER

Sensors and Actuators A 55 (1996) 43–47

SENSORS ACTUATORS A PHYSICAL

Parameter extraction of resistive thermal sensors

Yeong-Maw Chen *, Jin-Shown Shie, Thunter Hwang

Institute of Electro-Optical Engineering, National Chiao Tung University, 1001 Ta Hsueh Road, Hsinchu, Taiwan

Abstract

Obtaining thermal parameters is important in evaluating the performance of thermal microsensors. Two experimental methods are described here for the study of the pressure-dependent thermal behavior of the sensors: a bolometric method that utilizes a chopped light input to obtain a sensor frequency response, and deriving its thermal data therefrom; a d.c. electrical method that measures the heat required for balance under d.c. bias, and obtaining sensor information. The thermal conductance and capacitance, absorptance, as well as emissivity of a sensor can be extracted from the experimental measurements. These parameters provide the essential data for the electrothermal SPICE program in the related design simulations.

Keywords: Thermal sensors; Parameter extraction; Bolometric method; D.c. method

1. Introduction

In recent years, resistive thermal sensors utilizing microfabrication technology have been widely applied for transduction of various physical and chemical measurants; the bolometer for infrared sensing [1–4], the Pirani sensor for vacuum measurements [5,6], and sensors for detecting toxic gas contents [7,8], are just a few examples. Upon heating, these devices transduce specific measurants into electrical signals through the change of temperature-sensitive resistance. As a consequence, performance-related properties of the sensor, such as sensitivity and speed of response, depend strongly on its thermal characteristics; the most relevant of which are the thermal conductance and capacitance. Extracting the thermal parameters is hence important in evaluating these sensors, and is the objective of this report.

There have been many techniques reported to measure the thermal properties of thin films, examples of which are the d.c. method for polysilicon [9,10] and the a.c. method for nitride [11]. Here a method based on the bolometer principle is used, and when combined with a d.c. electrical method, the desired parameters of thermal sensors are derivable with reasonable accuracy, which constitute the essential data for the electrothermal SPICE simulation of the related devices [12–14].

2. The principle

In order to obtain a simpler analytical solution for interpreting the measured data, a resistive thermal sensor is operated with a constant-current (CC) bias circuit throughout the experiment.

In the d.c. electrical method, the static condition is held and no external power is provided except the device bias self-heating. The heat-balance condition then reads

$$G(\bar{T}-T_a)=P_e=I_b{}^2R_b=\langle I_bV_b\rangle \tag{1}$$

Here G is the lump thermal conductance; T_a and $\bar{T}$ are the ambient and average device temperature, respectively; P_e is the self-heating power; I_b and V_b are the current and voltage across a thermal sensor of resistance R_b, respectively. The angle brackets denote a quantity that is measurable by experiment.

In this study, platinum film is used as the sensing resistor, which has an excellent linear behavior to temperature that can be described by

$$R_b=R_{b0}[1+\alpha_0(T-T_0)]=\langle V_b/I_b\rangle \tag{2}$$

Here R_{b0} and α_0 are respectively the resistance and temperature coefficient (TCR) of the sensor with reference to a temperature T_0. In the static condition, T is replaced by the average quantity, $\bar{T}$, in Eq. (2). One notes that $R_b=\langle V_b/I_b\rangle$ is also measurable by experiment.

By combining the last two equations, the conductance G can be derived to give a result

* Corresponding author. Phone: +886 3 4891671. Fax: +886 35 716631. E-mail: u7924803@cc.nctu.edu.tw.

PII S0924-4247(96)01248-4

$$G=\frac{\langle I_b V_b\rangle R_{b0}\alpha_0}{\langle V_b/I_b\rangle - R_a} \tag{3}$$

with

$$R_a = R_{b0}[1+\alpha_0(T_a - T_0)] \tag{4}$$

as the sensor resistance measured at an ambient temperature T_a. With the d.c. electrical method, G can be calculated with the necessary experimental data listed in Eq. (3). One should note that the calculation is very sensitive to the ambient temperature variation, since the two resistance terms in the denominator of Eq. (3) are only slightly different. Therefore, it is necessary to monitor the true ambient temperature during experiments with the d.c. method.

In the bolometric method, the a.c. steady state condition is required. We use a lump heat-flow equation for the analysis [15], which reads

$$H\frac{dT}{dt} + G(T-T_a) = I_b{}^2 R_b + a\Phi$$
$$= I_b{}^2 R_b + a\Phi_m[1+\exp(j\omega t)] \tag{5}$$

where H is the thermal capacitance of a thermal sensor; a is its effective absorptance referred to the incident light spectrum [16]; and Φ_m is the modulation of optical power falling upon the sensor.

Substituting Eqs. (2) and (4) into Eq. (5) for a constant current I_b, then

$$H\frac{dT}{dt} + (G - I_b{}^2 R_{b0}\alpha_0)(T-T_a)$$
$$= (I_b{}^2 R_a + a\Phi_m) + a\Phi_m \exp(j\omega t) \tag{6}$$

The optical modulation causes a temperature perturbation close to the average temperature, i.e., $T=\bar{T}+\Delta T$. Putting the equality into Eq. (6) and deducting the static terms on both sides, one obtains

$$H\frac{d\Delta T}{dt} + (G - I_b{}^2 R_{b0}\alpha_0)\Delta T = a\Phi_m \exp(j\omega t) \tag{7}$$

Since the ambient temperature is a slow-varying function of time comparable to the optical modulation frequency ω, the a.c. method, unlike the d.c. method, is not sensitive to the ambient temperature drift. Eq. (7) can be solved for the spectral thermal responsivity R_T, which reads

$$R_T = \frac{a}{G - I_b{}^2 R_{b0}\alpha_0}\frac{1}{\sqrt{1+\omega^2\tau^2}} \ (^\circ C\ W^{-1}) \tag{8}$$

with

$$\tau = \frac{H}{G - I_b{}^2 R_{b0}\alpha_0} \tag{9}$$

as the effective thermal time constant. The voltage responsivity is derivable as follows

$$R_V = \frac{dV}{d\Phi} = \left(\frac{dV}{dR}\right)\left(\frac{dR}{dT}\right)\left(\frac{dT}{d\Phi}\right)$$
$$= (I_b)(R_{b0}\alpha_0)(R_T)$$
$$= \frac{R_{V0}}{\sqrt{1+\omega^2\tau^2}} \ (V\ W^{-1}) \tag{10}$$

which has a flatband responsivity

$$R_{V0} = \frac{aI_b R_{b0}\alpha_0}{G - I_b{}^2 R_{b0}\alpha_0} \tag{11}$$

To make Eq. (11) more interpretative to the experiment, we can rearrange it into

$$\log(R_{V0}{}^{-1} + a^{-1}I_b) = -\log I_b + \log\left(\frac{G}{aR_{b0}\alpha_0}\right) \tag{12}$$

If $R_{V0}{}^{-1} \gg a^{-1}I_b$, then a linear plot between $\log R_{V0}{}^{-1}$ and $\log I_b$ can be obtained with a slope of -1 and an intercept of $\log(G/aR_{b0}\alpha_0)$. According to Eq. (11), the above limitation is equivalent to

$$I_b \ll \sqrt{\frac{G}{2R_{b0}\alpha_0}} \tag{13}$$

From the intercept data, one can find the effective absorptance, a, with a known G obtained by the d.c. method. Alternately one can match two sets of G values obtained by the two methods, while using an estimated value of a. In the following, when the pressure-dependent behavior of a sensor conductance is analyzed, the latter approach is used.

The thermal capacitance, H, is also derivable from Eq. (9) when the effective thermal time constant, τ, is found by fitting the experimental data of spectral response with Eq. (10).

3. The experiment

To verify the above analysis, we have used a fabricated microbolometer as depicted in Fig. 1 [17], having a suspended glass-membrane structure, for the experiments. The membrane is supported by leads extended from corners of a v-grooved cavity. The platinum sensing element is coated on the membrane and passivated by PSG. A thin nichrome film

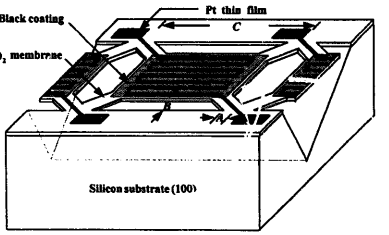

Fig. 1. Geometrical structure of a fabricated microbolometer.

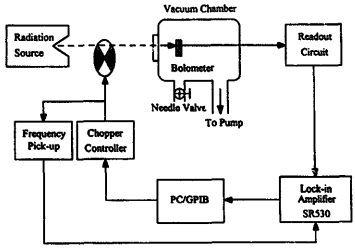

Fig. 2. The setup for characterizing the thermal microsensor experiments in a controlled vacuum environment.

is deposited on the top as the black coating for radiation absorption. The fabricated device has a TCR of 0.28% and an R_{b0} of 1145 Ω at 0°C reference.

As mentioned before in Eq. (3), the accuracy of G calculated by the d.c. electrical method is sensitive to the influence of ambient temperature. Hence a dummy sensor, not shown in Fig. 1, in close contact with the substrate without v-grooved floating is provided along with the sensor in order to measure accurately the substrate temperature, which is assumed to be close to ambient. We have found that without such an arrangement, the calculated G values in the d.c. method will give irreproducible and inconsistent results.

Fig. 2 shows the setup for measuring device responses in a controlled vacuum environment. In the bolometric method, a He–Ne laser is chopped into modulated light before falling upon the microbolometer that is set in a vacuum chamber. Signals from the sensor are fed to a low-noise amplifier and subsequently to a lock-in amplifier, which are then read by a PC through a GPIB interface. The device output is calibrated by a pyroelectric detector to obtain the absolute spectral responsivity. While in the d.c. electrical method, the chamber window is shielded from light input and the device is driven by a constant-current circuit alone. Voltages and currents across the sensor are measured accordingly under varying pressure conditions.

4. Results and discussion

For the bolometric method, spectral voltage responsivities were measured with varying bias currents and pressures. Their flatband response (R_{V0}) and the cutoff frequencies ($1/2\pi\tau$) were evaluated by fitting Eqs. (9) and (10). Fig. 3 shows the experimental plot of R_{V0}^{-1} versus I_b, in which the slope of the lines is indeed -1, as predicted by Eq. (12). Since the device has the smallest value of G around 5×10^{-6} W °C^{-1}, as shown in the following data (Fig. 4, low-pressure), this implies a limitation of $I_b \ll 0.88$ mA, according to Eq. (13). The effectiveness of Eq. (12) for the plot is thus confirmed.

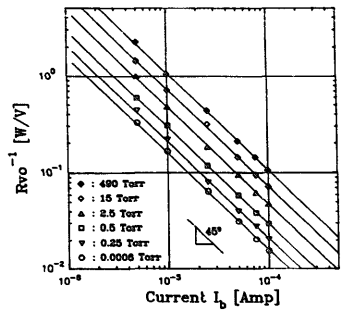

Fig. 3. Experimental R_{V0}^{-1} vs. I_b plot for determining the thermal conductance by the bolometric method.

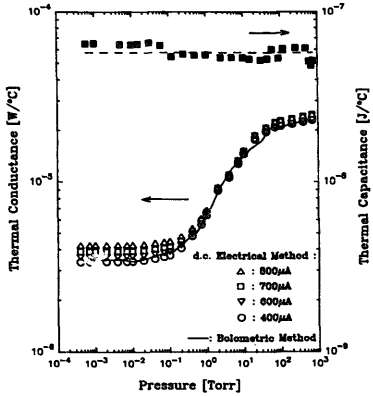

Fig. 4. The derived thermal conductances (hollow symbols) and thermal capacitance (solid squares) of a fabricated micro-thermal sensor as a function of vacuum pressure.

The G values derived from Fig. 3 are plotted as a function of the pressure (indicated in Fig. 4 by the solid curve), with a chosen absorptance value of 0.6. This curve is matched to the data calculated from the d.c. method with 400 μA bias current. However, data with other bias-current conditions deviated from the curve at the low-pressure regime; a larger bias current produces a higher conductance. This is due to the higher device temperature induced by the current, which increases the solid and radiative loss conductances included in G. This will be discussed in detail later.

Fig. 4 also shows the thermal capacitance H, obtained by the experimental fitting, which is basically insensitive to pressure, and can be considered as a constant.

The conductance G of a thermal device is formed by three loss mechanisms, namely the solid, gaseous and radiative

conductances, denoted by G_s, G_g and G_r, respectively. A detailed analysis for a membrane device similar to that shown in Fig. 1 has been reported by Weng and Shie [6]. For the solid conductance, leads are the bottleneck for heat loss. It is expressible empirically by [6]

$$G_s^{-1} = \frac{\gamma}{k_c d}\frac{B}{A} + r_0 \tag{14}$$

For our device, γ is a constant (0.24); d, B and A are the thickness (1.75 μm), projection length (16 μm) and width (8 μm) as shown in Fig. 1, respectively. r_0 is the spreading thermal resistance (5×10^4 °C W^{-1}) at the lead ends. k_c is the effective thermal conductivity of the leads, which is contributed by that of the four glass leads and the two metal-film leads.

The gaseous conductance is expressed as

$$G_g = \kappa P\left(\frac{P_{t1}}{P+P_{t1}} + \frac{P_{t2}}{P+P_{t2}}\right) \tag{15}$$

where κ is a constant related to the molecular properties of ambient gas, and P_{t1} and P_{t2} are the transition pressures on the lower and upper sides of the membrane, respectively. Physically, the transition pressure, which is inversely proportional to the effective distance from the membrane, denotes the separation of the viscous state from the molecular state in gaseous conduction [18]. The effective distance of the lower side is estimated by three-dimensional numerical calculation of the gas flux [6], and then the P_{t1} is adjusted by this distance. The P_{t2}, corresponding to the effect of upper side, is fitted by experimental data.

The radiative conductance is expressed as [6]

$$G_r = 2\varepsilon\sigma A_d(\bar{T}^2 + T_a^2)(\bar{T} + T_a) \tag{16}$$

with σ the Stefan–Boltzmann constant, A_d the sensor area (1.44×10^{-4} cm^2), and ε the apparent blackbody emissivity [16] of the membrane.

It is interesting to note that in Eqs. (14)–(16), G_s and G_g are not strong functions of the device temperature compared to G_r. At a higher pressure state, G_g is dominant in G with a larger value, which results in a lower device temperature. Therefore different bias currents cannot produce significant differences in the device temperature, and thus the radiation, and G is nearly independent of the bias current. However, at the low-pressure condition, G_g is reduced to a negligible value compared to the solid and radiative conductances. Hence the device temperature is raised significantly with the increased bias current, making the solid and radiation loss detectable in our experiment. We can assume that, for solid conductance, the effective thermal conductivity k_c of the leads in Eq. (14) depends linearly on temperature, that is

$$k_c = k_0 + k_1(T - 300\ \text{K}) \tag{17}$$

This assumption is reasonable, because the conductivity of a glass insulator is increased with temperature due to the increasing phonon number, according to Bose–Einstein statistics [19]. This relationship together with Eqs. (14) and (16) can be used to fit the low-pressure experimental data and derive the material parameters. Fig. 5 shows the results of the best fitting, which gives $\varepsilon = 0.6$, $k_0 = 8.5\times10^{-3}$ (W cm^{-1} °C^{-1}), and $k_1 = 4.5\times10^{-6}$ (W cm^{-1} °C^{-2}).

Table 1 summarizes the parameters of the measured devices extracted from the experiments. One should note that ε and a are based on different spectral references. a is referred to 6328 Å monochromatic wavelength, while ε is the spectral average at the sensor temperature, or the blackbody emissivity. Therefore, they are not necessarily identical as described by Kirchhoff's law [16].

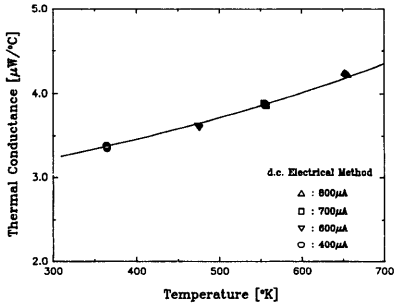

Fig. 5. Emissivity and thermal conductance fitting using Eqs. (14) and (16) with the low-pressure data of the d.c. electrical method.

5. Conclusions

Extraction of device parameters is useful in design and performance verification of thermal microsensors. It is also essential to provide such information for the electrothermal SPICE program in practical simulations. Two experimental

Table 1
The parameters of a fabricated microbolometer extracted by the experiments

κ (W torr^{-1} °C^{-1})	P_{t1} (torr)	P_{t2} (torr)	k_0 (W cm^{-1} °C^{-1})	k_1 (W cm^{-1} °C^{-2})	H (J °C^{-1})	a[a]	ε[b]
1.86×10^{-6}	10.5	1.12	8.5×10^{-3}	4.5×10^{-6}	5.74×10^{-8}	0.6	0.6

[a] Spectral absorptance [16] referred to He–Ne 6328 Å wavelength.
[b] Blackbody emissivity [16] at the membrane temperature.

methods have been introduced in detail in this study. Their effectiveness has been proved by the comparison of the experimental data with the analytical formulae. The d.c. electrical method is sensitive to the ambient temperature variation, which must be measured accurately during the experiment. These methods provide additional information for the effective absorptance and apparent emissivity, which otherwise would be very difficult to measure directly.

Acknowledgements

The authors wish to express their appreciation to Opto Tech Corporation in Science-based Industry Park of Hsinchu, Taiwan, for the technical support on the device processing. They are indebted to Dr P.K. Weng for preparing the samples. This project is supported by the National Science Council of the Republic of China under project contract No. NSC-85-2215-E-009-040.

References

[1] J.S. Shie and P.K. Weng, Fabrication of micro-bolometer on silicon substrate by anisotropic etching technique, *Tech. Digest, 6th Int. Conf. Solid-State Sensors and Actuators (Transducers '91), San Francisco, CA, USA, 24–28 June, 1991*, pp. 627–630.

[2] R.A. Wood, C.J. Han and P.W. Kruse, Integrated uncooled infrared detector imaging arrays, *Tech. Digest, IEEE Solid-State Sensor and Actuator Workshop, Hilton Head, SC, USA, June 1992*, pp. 132–135.

[3] T. Mori, T. Kudoh, K. Komatsu and M. Kimura, Vacuum-encapsulated thermistor bolometer type miniature infrared sensor, *IEEE Proc. MEMS, Jan. 1994*, pp. 257–262.

[4] A. Tanaka, S. Matsumoto, N. Tsukamoto, S. Itoh, T. Endoh, A. Nakazoto, Y. Kumazawa, M. Hijikawa, H. Gotoh, T. Tanaka and N. Teranishi, Silicon IC process compatible bolometer infrared focal plane array, *Tech. Digest, 8th Int. Conf. Solid-State Sensors and Actuators (Transducers '95)/Eurosensors IX, Stockholm, Sweden, 25–29 June, 1995*, Vol. 2, pp. 632–635.

[5] C.H. Mastrangelo and R.S. Muller, Microfabricated thermal absolute-pressure sensor with on-chip digital front-end processor, *IEEE J. Solid-State Circuits, 26* (1991) 1998–2007.

[6] P.K. Weng and J.S. Shie, Micro-Pirani vacuum gauge, *Rev. Sci. Instrum., 65* (1994) 492–499.

[7] P.T. Moseley, *Solid State Gas Sensors*, Adam Hilger, Bristol, UK, 1987, Ch. 4.

[8] N. Najafi, K.D. Wise and J.W. Schwank, A micromachined ultra-thin-film gas detector, *IEEE Trans. Electron Devices, 41* (1994) 1770–1777.

[9] F. Volklein and H. Baltes, A microstructure for measurement of thermal conductivity of polysilicon thin films, *J. Microelectromech. Syst., 1* (1992) 193–196.

[10] O.M. Paul, J. Korvink and H. Baltes, Determination of the thermal conductivity of CMOS IC polysilicon, *Sensors and Actuators A, 41–42* (1994) 161–164.

[11] X. Zhang and C.P. Grigoropoulos, Thermal conductivity and diffusivity of free-standing silicon nitride thin films, *Rev. Sci. Instrum., 66* (1995) 1115–1120.

[12] J.S. Shie, Y.M. Chen, M. Ou-Yang and B.C.S. Chou, Characterization and modeling of metal-film microbolometer, to be published.

[13] N.R. Swart and A. Nathan, Flow-rate microsensor modelling and optimization using SPICE, *Sensors and Actuators A, 34* (1992) 109–122.

[14] S.S. Lee and D.J. Allstot, Electro-thermal simulation of integrated circuit, *IEEE J. Solid-State Circuits, 28* (1993) 1283–1293.

[15] W. Budde, *Optical Radiation Measurements*, Vol. 4, *Physical Detectors of Optical Radiation*, Academic Press, New York, 1983, Ch. 4.

[16] R.D. Hudson, *Infrared System Engineering*, Wiley, New York, 1969, Ch. 2, pp. 39–53.

[17] J.S. Shie and P.K. Weng, Design considerations of metal-film bolometer with micromachined floating membrane, *Sensors and Actuators A, 33* (1992) 183–189.

[18] S. Dushman, *Scientific Foundations of Vacuum Technique*, Wiley, New York, 2nd edn., 1962, Ch.1.

[19] C. Kittel, *Introduction to Solid State Physics*, John Wiley, New York, 1971, Ch. 6.

Biographies

Yeong-Maw Chen received his B.Sc. degree in physics from National Central University of Taiwan in 1981, and his masters degree in electro-optical engineering from National Chiao Tung University in 1983. Since then he has been working in CSIST on microwave system design. He is currently a Ph.D. candidate in the Institute of Electro-Optical Engineering of National Chiao Tung University, majoring in uncooled infrared detection.

Jin-Shwon Shie is currently a professor of the Institute of Electro-Optical Engineering of National Chiao Tung University. He earned his B.S.E.E. degree from National Cheng Kung University of Taiwan in 1965, and his M.S.E.E. degree from National Chiao Tung University in 1968. In 1972 he received his Ph.D. degree from the Department of Materials Science, SUNY at Stony Brook, USA. His present interest is in the field of photodetection, particularly in the fabrication of uncooled infrared FPA detectors and system design.

Thunter Hwang received his bachelors degree in electrical engineering from National Cheng Kung University of Taiwan in 1984, and his masters degree in electro-optical engineering from National Chiao Tung University in 1995. He is currently working in the research division of Philips Electronics Industries (Taiwan) Ltd. at Hsinchu Science-based Industrial Park, Taiwan.